

## X-ray Resonant Exchange Scattering: Polarization Dependence and Correlation Functions

J. P. HILL<sup>a\*</sup> AND D. F. MCMORROW<sup>b</sup>

<sup>a</sup>Department of Physics, Brookhaven National Laboratory, Upton, NY 11973, USA, and <sup>b</sup>Department of Solid State Physics, Risø National Laboratory, DK-4000 Roskilde, Denmark. E-mail: john@solids.phy.bnl.gov

(Received 27 April 1995; accepted 2 October 1995)

### Abstract

The cross section for X-ray resonant exchange scattering is reformulated in terms of linear polarization states perpendicular and parallel to the scattering plane, a basis particularly well suited to synchrotron X-ray diffraction experiments. The explicit polarization dependence of the terms is calculated for the electric dipole and quadrupole contributions. This expression, in turn, is rewritten in an orthonormal basis to highlight the dependence of the cross section on each component of the magnetic moment. This has the benefit of providing an empirically useful expression for the cross section. Diffraction patterns from a few simple magnetic structures are calculated. Finally, the correlation function measured at each resonant harmonic is derived.

### 1. Introduction

Large resonant enhancements of the X-ray magnetic scattering cross section were first reported in Ho by Gibbs *et al.* (1988), who observed a significant increase in the signal on tuning the incident X-ray energy through the  $L_{III}$ -absorption edge. The enhancement was explained using an atomic picture of the electric multipole transitions by Hannon, Trammel, Blume & Gibbs (1988). Subsequently, larger enhancements were observed at the  $M$  edges of the actinides (Isaacs *et al.*, 1989). The large signal rates produced at resonance have allowed a variety of previously inaccessible problems to be studied with this technique and a number of elegant experiments have now been performed (Thurston *et al.*, 1993; Gibbs *et al.*, 1991; Isaacs *et al.*, 1990; Tang *et al.*, 1992; de Bergevin *et al.*, 1992). The non-resonant cross section (*i.e.* that for incident X-ray energies far from any absorption edges) is well understood (Blume, 1985) and has been written in a form useful to practitioners in the field (Blume & Gibbs, 1988). However, the resonant terms in the cross section were originally formulated using vector spherical harmonics, a notation borrowed from resonance  $\gamma$ -ray scattering (Trammel, 1962; Trammel & Hannon, 1969) and are less transparent in terms of their polarization dependence and sensitivity to individual components of the magnetic moment.

The purpose of this paper is first to reformulate the cross section of Hannon *et al.* (1988) using the same basis as that of Blume & Gibbs (1988), which is a natural choice for synchrotron X-ray scattering experiments. In particular, we rewrite the cross section in the form of  $2 \times 2$  matrices in a basis whose components are perpendicular and parallel to the scattering plane. By convention, these are labeled  $\sigma$  and  $\pi$  polarizations, respectively. This representation highlights the polarization dependence of each term in the cross section in a manner which it is hoped will be of use to experimenters. We further decompose the magnetic moment of the scatterer into orthogonal components to elucidate how each component contributes to the scattering. The resulting expression is a particularly useful one for resonant magnetic scattering. Diffraction patterns from simple magnetic structures are then calculated to illustrate the ease with which this can be done.

In the second half of this paper, we derive the correlation functions measured at the various diffraction harmonics observed in incommensurate magnetic structures at resonance. This has particular application to recent experiments in holmium in which non-mean-field scaling was observed in the temperature dependence of the resonant harmonics (Helgesen *et al.*, 1994).

### 2. The cross section

Following Hannon *et al.* (1988), we begin by writing the total coherent elastic scattering amplitude for scattering from a magnetic ion:

$$f = f_0 + f' + if'' + f_{\text{spin}} \quad (1)$$

Here,  $f_0 \propto Zr_0$  is the Thomson charge scattering amplitude and  $f_{\text{spin}}$  the non-resonant spin-dependent magnetic scattering amplitude. Far from resonance,  $f'$  and  $f''$  contribute terms proportional to the orbital and spin angular momentum, and the total non-resonant magnetic scattering amplitude is (Blume, 1985; Blume & Gibbs, 1988)

$$f_{\text{non-res}}^{(\text{mag})} = ir_0(\hbar\omega/mc^2)f_D[\frac{1}{2}\mathbf{L}(\mathbf{Q}) \cdot \mathbf{A} + \mathbf{S}(\mathbf{Q}) \cdot \mathbf{B}], \quad (2)$$

where  $\mathbf{L}(\mathbf{Q})$  and  $\mathbf{S}(\mathbf{Q})$  are the Fourier transforms of the

atomic orbital and spin magnetic densities, respectively.  $\mathbf{A} = 2(1 - \hat{\mathbf{k}} \cdot \hat{\mathbf{k}}')(\hat{\boldsymbol{\varepsilon}}' \times \hat{\boldsymbol{\varepsilon}}) - (\hat{\mathbf{k}} \times \hat{\boldsymbol{\varepsilon}})(\hat{\mathbf{k}} \cdot \hat{\boldsymbol{\varepsilon}}') + (\hat{\mathbf{k}}' \times \hat{\boldsymbol{\varepsilon}}')(\hat{\mathbf{k}} \cdot \hat{\boldsymbol{\varepsilon}})$  and  $\mathbf{B} = (\hat{\boldsymbol{\varepsilon}}' \times \hat{\boldsymbol{\varepsilon}}) + (\hat{\mathbf{k}}' \times \hat{\boldsymbol{\varepsilon}}')(\hat{\mathbf{k}} \cdot \hat{\boldsymbol{\varepsilon}}) - (\hat{\mathbf{k}} \times \hat{\boldsymbol{\varepsilon}})(\hat{\mathbf{k}} \cdot \hat{\boldsymbol{\varepsilon}}') - (\hat{\mathbf{k}}' \times \hat{\boldsymbol{\varepsilon}}') \times (\hat{\mathbf{k}} \times \hat{\boldsymbol{\varepsilon}})$ , where  $\boldsymbol{\varepsilon}$  and  $\boldsymbol{\varepsilon}'$  are the incident and scattered polarization vectors, respectively, and  $\mathbf{k}$  and  $\mathbf{k}'$  are the incident and scattered wave vectors, respectively.  $\mathbf{Q} = \mathbf{k}' - \mathbf{k}$  is the wave-vector transfer and  $f_D$  is the Debye-Waller factor. The resonant processes discussed here enter the cross section through  $f'$  and  $f''$ . Although both electric and magnetic multipole transitions contribute, the electric dipole and quadrupole transitions are the dominant processes, if allowed. The magnetic multipole contributions are smaller by a factor  $\hbar\omega/mc^2$  (Hannon *et al.*, 1988) ( $\leq 1/60$  for typical X-ray edges) and are not considered here.

For the electric  $2^L$ -pole resonance in a magnetic ion, the resonant contribution to the coherent scattering amplitude is (Hannon *et al.*, 1988)

$$f_{\text{EL}}^e(\omega) = (4\pi/|k|)f_D \sum_{M=-L}^L [\hat{\boldsymbol{\varepsilon}}'^* \cdot \mathbf{Y}_{LM}^{(e)}(\hat{\mathbf{k}}') \mathbf{Y}_{LM}^{(e)*}(\hat{\mathbf{k}}) \cdot \hat{\boldsymbol{\varepsilon}}] F_{LM}^{(e)}(\omega), \quad (3)$$

where  $\mathbf{Y}_{LM}^{(e)}(\hat{\mathbf{k}})$  are vector spherical harmonics. The strength of the resonance is determined by the factor  $F_{LM}$ , which, in turn, is determined by atomic properties:

$$F_{LM}^{(e)}(\omega) = \sum_{\alpha, \eta} [P_\alpha P_\alpha(\eta) \Gamma_x(\alpha M \eta; \text{EL}) / \Gamma(\eta)] / [x(\alpha, \eta) - i]. \quad (4)$$

Here,  $\eta$  is the excited state of the ion and  $\alpha$  the initial state.  $P_\alpha$  is the probability of the ion existing in the initial state  $\alpha$  and  $P_\alpha(\eta)$  the probability for a transition from  $\alpha$  to a final state  $\eta$ . It is determined by overlap integrals between the two states  $\alpha$  and  $\eta$ .  $\Gamma_x/\Gamma$  is the ratio of the partial line width of the excited state due to a pure electric  $2^L$ -pole (EL) radiative decay to that due to all processes, both radiative and non-radiative (including, for example, Auger decay). Finally,  $x = (E_\eta - E_\alpha - \hbar\omega)/(\Gamma/2)$  is the deviation from the resonance condition in units of the total half-width. [An alternative derivation of this cross section based on symmetry arguments has recently been presented by Blume (1994).] This form of the scattering amplitude is valid for isotropic systems in which the symmetry is only broken by the magnetic moment. The application of the symmetries of a particular point group produced by the local environment will alter the allowed terms. Such effects were used to explain the azimuthal dependence of resonant charge scattering at Bragg forbidden positions in  $\text{Fe}_2\text{O}_3$ , which has a  $C_3$  point group at the Fe site (Finkelstein, Shen & Shastri, 1992; Finkelstein, Hamrick & Shen, 1993; Hamrick, 1994; Carra & Thole, 1994). M. Blume (unpublished work) has considered a number of common point groups and the case of the cubic group has been considered in detail by Rennert (1993).

### 2.1. Electric dipole transitions (E1)

Electric dipole transitions usually dominate the resonant magnetic cross section and are the simplest to calculate. An example of such a transition is the  $2p_{3/2} \rightarrow 5d_{1/2}$  transition of Ho, which occurs at the  $L_{\text{III}}$ -absorption edge. At such a transition, the vector spherical harmonics can be written (Berestetskii, Lifshitz & Pitaevskii, 1971), for  $L = 1$ ,  $M = \pm 1$ :

$$[\hat{\boldsymbol{\varepsilon}}' \cdot \mathbf{Y}_{1\pm 1}(\hat{\mathbf{k}}') \mathbf{Y}_{1\pm 1}^*(\hat{\mathbf{k}}) \cdot \hat{\boldsymbol{\varepsilon}}] = (3/16\pi)[\hat{\boldsymbol{\varepsilon}}' \cdot \hat{\boldsymbol{\varepsilon}} \mp i(\hat{\boldsymbol{\varepsilon}}' \times \hat{\boldsymbol{\varepsilon}}) \cdot \hat{\mathbf{z}}_n - (\hat{\boldsymbol{\varepsilon}}' \cdot \hat{\mathbf{z}}_n)(\hat{\boldsymbol{\varepsilon}} \cdot \hat{\mathbf{z}}_n)]; \quad (5)$$

and, for  $L = 1$ ,  $M = 0$ ;

$$[\hat{\boldsymbol{\varepsilon}}' \cdot \mathbf{Y}_{10}(\hat{\mathbf{k}}') \mathbf{Y}_{10}^*(\hat{\mathbf{k}}) \cdot \hat{\boldsymbol{\varepsilon}}] = (3/8\pi)[(\hat{\boldsymbol{\varepsilon}}' \cdot \hat{\mathbf{z}}_n)(\hat{\boldsymbol{\varepsilon}} \cdot \hat{\mathbf{z}}_n)]; \quad (6)$$

where  $\hat{\mathbf{z}}_n$  is a unit vector in the direction of the magnetic moment of the  $n$ th ion. Thus,

$$f_{nE1}^{\text{XRES}} = [(\hat{\boldsymbol{\varepsilon}}' \cdot \hat{\boldsymbol{\varepsilon}})F^{(0)} - i(\hat{\boldsymbol{\varepsilon}}' \times \hat{\boldsymbol{\varepsilon}}) \cdot \hat{\mathbf{z}}_n F^{(1)} + (\hat{\boldsymbol{\varepsilon}}' \cdot \hat{\mathbf{z}}_n)(\hat{\boldsymbol{\varepsilon}} \cdot \hat{\mathbf{z}}_n)F^{(2)}] \quad (7)$$

with

$$F^{(0)} = (3/4k)[F_{11} + F_{1-1}] \quad (8)$$

$$F^{(1)} = (3/4k)[F_{11} - F_{1-1}] \quad (9)$$

$$F^{(2)} = (3/4k)[2F_{10} - F_{11} - F_{1-1}]. \quad (10)$$

The first term of (7) simply contributes to the charge Bragg peak, since it contains no dependence on the magnetic moment. In an incommensurate antiferromagnet, the second term produces first-harmonic magnetic satellites and the third term, which contains two powers of the magnetic moment, produces the second-harmonic magnetic satellites. The amplitude of the scattering is controlled by the overlap integrals, making it possible, at least in principle, to observe very small magnetic moments. For example, Isaacs *et al.* have observed scattering from  $\text{URu}_2\text{Si}_2$  with an ordered moment of only  $0.02\mu_B$ , by tuning to the  $M_{\text{IV}}$ -absorption edge of U (Isaacs *et al.*, 1990), for which there is a large overlap between initial and excited states.

We now write the dipole operator of (7) as a  $2 \times 2$  matrix, with the polarization states chosen either parallel or perpendicular to the scattering plane as shown in Fig. 1. This representation was first used by de Bergevin and Brunel in their derivation of the non-resonant magnetic cross section for X-ray scattering (de Bergevin & Brunel, 1981). It is easy to see that the first term connects only states for which the polarization is unchanged, *i.e.* an  $\hat{\boldsymbol{\varepsilon}}_{\parallel}$  photon is scattered into an  $\hat{\boldsymbol{\varepsilon}}'_{\parallel}$  (so called  $\pi \rightarrow \pi$  scattering) and  $\hat{\boldsymbol{\varepsilon}}_{\perp} \rightarrow \hat{\boldsymbol{\varepsilon}}'_{\perp}$  (or  $\sigma \rightarrow \sigma$  scattering). Thus, this matrix is diagonal with elements  $\hat{\boldsymbol{\varepsilon}}'_{\perp} \cdot \hat{\boldsymbol{\varepsilon}}_{\perp} = 1$  and  $\hat{\boldsymbol{\varepsilon}}'_{\parallel} \cdot \hat{\boldsymbol{\varepsilon}}_{\parallel} = \cos 2\theta = \hat{\mathbf{k}} \cdot \hat{\mathbf{k}}'$  and

$$\hat{\boldsymbol{\varepsilon}}' \cdot \hat{\boldsymbol{\varepsilon}} = \begin{pmatrix} 1 & 0 \\ 0 & \hat{\mathbf{k}}' \cdot \hat{\mathbf{k}} \end{pmatrix}. \quad (11)$$

On the other hand, the second term allows  $\sigma \leftrightarrow \pi$  scattering as well as  $\pi \rightarrow \pi$  scattering, but  $\sigma \rightarrow \sigma$  scattering is forbidden and the matrix representation is

$$(\hat{\epsilon}' \times \hat{\epsilon}) \cdot \hat{z}_n = \begin{pmatrix} 0 & \hat{\mathbf{k}} \\ -\hat{\mathbf{k}}' & \hat{\mathbf{k}}' \times \hat{\mathbf{k}} \end{pmatrix} \cdot \hat{z}_n, \quad (12)$$

where the off-diagonal elements are  $\hat{\epsilon}'_{\parallel} \times \hat{\epsilon}_{\perp} = -\hat{\mathbf{k}}'$  and  $\hat{\epsilon}'_{\perp} \times \hat{\epsilon}_{\parallel} = \hat{\mathbf{k}}$ . The matrix representation of the third term is obtained in a similar fashion. The identities

$$\begin{aligned} \hat{\mathbf{k}} \cdot \hat{\mathbf{k}}' &= \cos 2\theta \\ 1 - (\hat{\mathbf{k}} \cdot \hat{\mathbf{k}}')^2 &= \sin^2 2\theta \\ \hat{\mathbf{k}}' \times \hat{\mathbf{k}} &= -\hat{U}_2 \sin 2\theta \\ \hat{\mathbf{k}} + \hat{\mathbf{k}}' &= 2\hat{U}_1 \cos \theta \\ \hat{\mathbf{k}} - \hat{\mathbf{k}}' &= 2\hat{U}_3 \sin \theta \\ \hat{z}_n &= \sum_i (\hat{U}_i \cdot \hat{z}_n) \hat{U}_i \end{aligned} \quad (13)$$

are used to obtain the final result:

$$\begin{aligned} f_{n\hat{\epsilon}1}^{\text{XRES}} &= F^{(0)} \begin{pmatrix} 1 & 0 \\ 0 & \hat{\mathbf{k}}' \cdot \hat{\mathbf{k}} \end{pmatrix} - iF^{(1)} \begin{pmatrix} 0 & \hat{\mathbf{k}} \cdot \hat{z}_n \\ -\hat{\mathbf{k}}' \cdot \hat{z}_n & (\hat{\mathbf{k}}' \times \hat{\mathbf{k}}) \cdot \hat{z}_n \end{pmatrix} \\ &+ \{F^{(2)}/[1 - (\hat{\mathbf{k}}' \cdot \hat{\mathbf{k}})^2]\} \\ &\times \begin{pmatrix} [(\hat{\mathbf{k}}' \times \hat{\mathbf{k}}) \cdot \hat{z}_n]^2 & [\hat{\mathbf{k}}' \cdot \hat{z}_n - (\hat{\mathbf{k}} \cdot \hat{\mathbf{k}}')\hat{\mathbf{k}} \cdot \hat{z}_n](\hat{\mathbf{k}}' \times \hat{\mathbf{k}}) \cdot \hat{z}_n \\ [(\hat{\mathbf{k}} \cdot \hat{\mathbf{k}}')\hat{\mathbf{k}}' \cdot \hat{z}_n - \hat{\mathbf{k}} \cdot \hat{z}_n](\hat{\mathbf{k}}' \times \hat{\mathbf{k}}) \cdot \hat{z}_n & (\hat{\mathbf{k}} \cdot \hat{\mathbf{k}}')[(\hat{\mathbf{k}} \cdot \hat{z}_n)^2 + (\hat{\mathbf{k}}' \cdot \hat{z}_n)^2] \\ & - [1 + (\hat{\mathbf{k}} \cdot \hat{\mathbf{k}}')^2][(\hat{\mathbf{k}} \cdot \hat{z}_n)(\hat{\mathbf{k}}' \cdot \hat{z}_n)] \end{pmatrix}. \end{aligned} \quad (14)$$

A similar expression has also been obtained by Pengra, Thoft, Wulff, Feidenhans'l & Bohr (1994).

Next, we resolve each of the vectors  $\hat{\mathbf{k}}$ ,  $\hat{\mathbf{k}}'$  and  $\hat{z}_n$  into their components along  $\hat{U}_1$ ,  $\hat{U}_2$  and  $\hat{U}_3$ , the coordinate system defined with respect to the diffraction plane (Fig. 1). This results in the following expression for the resonant dipole scattering amplitude:

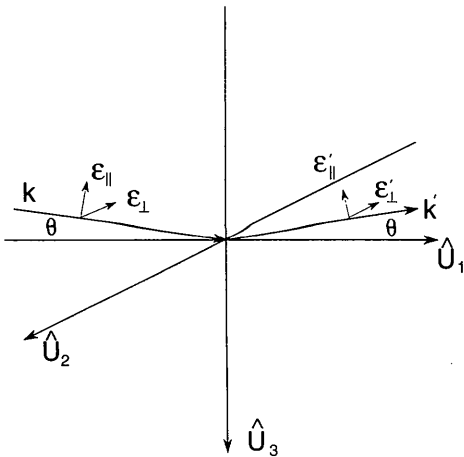


Fig. 1. The coordinate system used in calculating the polarization dependences.  $\theta$  is the Bragg angle.

$$\begin{aligned} f_{n\hat{\epsilon}1}^{\text{XRES}} &= F^{(0)} \begin{pmatrix} 1 & 0 \\ 0 & \cos 2\theta \end{pmatrix} - iF^{(1)} \begin{pmatrix} 0 & z_1 \cos \theta + z_3 \sin \theta \\ z_3 \sin \theta - z_1 \cos \theta & -z_2 \sin 2\theta \end{pmatrix} \\ &+ F^{(2)} \begin{pmatrix} z_2^2 & \\ +z_2(z_1 \sin \theta + z_3 \cos \theta) & -\cos^2 \theta (z_1^2 \tan^2 \theta + z_3^2) \end{pmatrix}, \end{aligned} \quad (15)$$

where  $\theta$  is the Bragg angle. From (15), it is possible to see which components of the magnetic moment contribute to the scattering for a given experimental geometry and, as we shall show in the next section, this is all that is required in many experiments. However, if a detailed comparison is to be made between (15) and a data set, then it is necessary to compute the magnitude of the coefficients  $F_{LM}$ . This is beyond the scope of this work, but the coefficients have been evaluated by Hamrick (1994) for several rare-earth elements.

## 2.2. Electric quadrupole transitions (E2)

We now carry out a similar procedure for the quadrupole contribution to the resonant cross section. An example of such a transition is the  $2p_{3/2} \leftrightarrow 4f$  transition at the  $L_{\text{III}}$  edge of Ho. While the scattering from such processes is typically weaker than that due to electric dipole transitions, it can be significant. For example, in an incommensurate antiferromagnet, the quadrupole terms produce two extra resonant harmonics. These have been observed experimentally (see, for example, Gibbs *et al.*, 1988) and it is an interesting question as to what magnetic properties are being probed at these harmonics. It is hoped that the results of this section will allow such questions to be answered.

We begin, as before, with the expansion of the vector spherical harmonics (Hannon *et al.*, 1988; Hamrick, 1990). For the  $L = 2$  case, 13 distinct terms are produced of various orders in the magnetic moment:

order zero

$$+(\hat{\mathbf{k}}' \cdot \hat{\mathbf{k}})(\hat{\epsilon}' \cdot \hat{\epsilon})F_{E2}^{(0)};$$

order one

$$-i[(\hat{\mathbf{k}}' \cdot \hat{\mathbf{k}})(\hat{\epsilon}' \times \hat{\epsilon}) \cdot \hat{z}_n + (\hat{\epsilon}' \cdot \hat{\epsilon})(\hat{\mathbf{k}}' \times \hat{\mathbf{k}}) \cdot \hat{z}_n]F_{E2}^{(1)};$$

order two

$$\begin{aligned} &+ [(\hat{\mathbf{k}}' \cdot \hat{\mathbf{k}})(\hat{\epsilon}' \cdot \hat{z}_n)(\hat{\epsilon} \cdot \hat{z}_n) \\ &+ (\hat{\epsilon}' \cdot \hat{\epsilon})(\hat{\mathbf{k}}' \cdot \hat{z}_n)(\hat{\mathbf{k}} \cdot \hat{z}_n)](F_{E2}^{(2)} - F_{E2}^{(0)}) \\ &+ [(\hat{\epsilon}' \cdot \hat{\mathbf{k}})(\hat{\mathbf{k}}' \cdot \hat{z}_n)(\hat{\epsilon} \cdot \hat{z}_n) + (\hat{\mathbf{k}}' \cdot \hat{\epsilon})(\hat{\epsilon}' \cdot \hat{z}_n)(\hat{\mathbf{k}} \cdot \hat{z}_n)]F_{E2}^{(2)} \\ &- [(\hat{\mathbf{k}}' \times \hat{\mathbf{k}}) \cdot \hat{z}_n(\hat{\epsilon}' \times \hat{\epsilon}) \cdot \hat{z}_n]F_{E2}^{(0)}; \end{aligned}$$

order three

$$\begin{aligned} &-i[(\hat{\mathbf{k}}' \cdot \hat{z}_n)(\hat{\mathbf{k}} \cdot \hat{z}_n)(\hat{\epsilon}' \times \hat{\epsilon}) \cdot \hat{z}_n \\ &+ (\hat{\epsilon}' \cdot \hat{z}_n)(\hat{\epsilon} \cdot \hat{z}_n)(\hat{\mathbf{k}}' \times \hat{\mathbf{k}}) \cdot \hat{z}_n](F_{E2}^{(3)} - F_{E2}^{(1)}) \\ &-i[(\hat{\epsilon}' \cdot \hat{z}_n)(\hat{\mathbf{k}} \cdot \hat{z}_n)(\hat{\mathbf{k}}' \times \hat{\epsilon}) \cdot \hat{z}_n \\ &+ (\hat{\mathbf{k}}' \cdot \hat{z}_n)(\hat{\epsilon} \cdot \hat{z}_n)(\hat{\epsilon}' \times \hat{\mathbf{k}}) \cdot \hat{z}_n]F_{E2}^{(3)}; \end{aligned}$$

order four

$$+(\hat{\mathbf{k}}' \cdot \hat{\mathbf{z}}_n)(\hat{\mathbf{k}} \cdot \hat{\mathbf{z}}_n)(\hat{\mathbf{e}}' \cdot \hat{\mathbf{z}}_n)(\hat{\mathbf{e}} \cdot \hat{\mathbf{z}}_n)F_{E2}^{(4)},$$

where

$$\begin{aligned} F_{E2}^{(0)} &= (5/4k)[F_{22} + F_{2-2}] \\ F_{E2}^{(1)} &= (5/4k)[F_{22} - F_{2-2}] \\ F_{E2}^{(2)} &= (5/4k)[F_{21} + F_{2-1}] \\ F_{E2}^{(3)} &= (5/4k)[F_{21} - F_{2-1}] \\ F_{E2}^{(4)} &= (5/4k)[F_{22} + F_{2-2} - 4F_{21} - 4F_{2-1} + 6F_{20}]. \end{aligned} \quad (16)$$

We now write these terms in the matrix representation of the previous section. The algebra is straightforward, if somewhat tedious. The following result for the polarization dependence of the resonant electric quadrupole terms is obtained:

$$\begin{aligned} f_{nE2}^{\text{XRES}} &= F_{E2}^{(0)} \begin{pmatrix} (\hat{\mathbf{k}} \cdot \hat{\mathbf{k}}') & 0 \\ 0 & (\hat{\mathbf{k}} \cdot \hat{\mathbf{k}}')^2 \end{pmatrix} \\ &\quad - iF_{E2}^{(1)} \begin{pmatrix} (\hat{\mathbf{k}}' \times \hat{\mathbf{k}}) \cdot \hat{\mathbf{z}}_n & (\hat{\mathbf{k}}' \cdot \hat{\mathbf{k}})(\hat{\mathbf{k}} \cdot \hat{\mathbf{z}}_n) \\ -(\hat{\mathbf{k}}' \cdot \hat{\mathbf{k}})(\hat{\mathbf{k}}' \cdot \hat{\mathbf{z}}_n) & 2(\hat{\mathbf{k}}' \cdot \hat{\mathbf{k}})(\hat{\mathbf{k}}' \times \hat{\mathbf{k}}) \cdot \hat{\mathbf{z}}_n \end{pmatrix} \\ &\quad + \frac{(F_{E2}^{(2)} - F_{E2}^{(0)})(\hat{\mathbf{k}}' \cdot \hat{\mathbf{k}})}{1 - (\hat{\mathbf{k}}' \cdot \hat{\mathbf{k}})^2} \begin{pmatrix} M_{21}^2 & M_{12}^2 \\ M_{21}^2 & M_{22}^2 \end{pmatrix} \\ &\quad + F_{E2}^{(2)} \begin{pmatrix} 0 & (\hat{\mathbf{k}}' \times \hat{\mathbf{k}}) \cdot \hat{\mathbf{z}}_n(\hat{\mathbf{k}} \cdot \hat{\mathbf{z}}_n) \\ -(\hat{\mathbf{k}}' \times \hat{\mathbf{k}}) \cdot \hat{\mathbf{z}}_n(\hat{\mathbf{k}}' \cdot \hat{\mathbf{z}}_n) & 2(\hat{\mathbf{k}} \cdot \hat{\mathbf{k}}')(\hat{\mathbf{k}}' \cdot \hat{\mathbf{z}}_n)(\hat{\mathbf{k}} \cdot \hat{\mathbf{z}}_n) \\ & -(\hat{\mathbf{k}}' \cdot \hat{\mathbf{z}}_n)^2 - (\hat{\mathbf{k}} \cdot \hat{\mathbf{z}}_n)^2 \end{pmatrix} \\ &\quad - F_{E2}^{(0)} \begin{pmatrix} 0 & (\hat{\mathbf{k}}' \times \hat{\mathbf{k}}) \cdot \hat{\mathbf{z}}_n(\hat{\mathbf{k}} \cdot \hat{\mathbf{z}}_n) \\ -(\hat{\mathbf{k}}' \times \hat{\mathbf{k}}) \cdot \hat{\mathbf{z}}_n(\hat{\mathbf{k}}' \cdot \hat{\mathbf{z}}_n) & [(\hat{\mathbf{k}}' \times \hat{\mathbf{k}}) \cdot \hat{\mathbf{z}}_n]^2 \end{pmatrix} \\ &\quad - \frac{i(F_{E2}^{(3)} - F_{E2}^{(1)})}{1 - (\hat{\mathbf{k}}' \cdot \hat{\mathbf{k}})^2} \begin{pmatrix} {}^1M_{11}^3 & {}^1M_{12}^3 \\ {}^1M_{21}^3 & {}^1M_{22}^3 \end{pmatrix} - \frac{iF_{E2}^{(3)}}{1 - (\hat{\mathbf{k}}' \cdot \hat{\mathbf{k}})^2} \begin{pmatrix} {}^2M_{11}^3 & {}^2M_{12}^3 \\ {}^2M_{21}^3 & {}^2M_{22}^3 \end{pmatrix} \\ &\quad + \frac{F_{E2}^{(4)}(\hat{\mathbf{k}}' \cdot \hat{\mathbf{z}}_n)(\hat{\mathbf{k}} \cdot \hat{\mathbf{z}}_n)}{1 - (\hat{\mathbf{k}}' \cdot \hat{\mathbf{k}})^2} \\ &\quad \times \begin{pmatrix} [(\hat{\mathbf{k}}' \times \hat{\mathbf{k}}) \cdot \hat{\mathbf{z}}_n]^2 & [\hat{\mathbf{k}}' \cdot \hat{\mathbf{z}}_n - (\hat{\mathbf{k}} \cdot \hat{\mathbf{k}}')\hat{\mathbf{k}} \cdot \hat{\mathbf{z}}_n](\hat{\mathbf{k}}' \times \hat{\mathbf{k}}) \cdot \hat{\mathbf{z}}_n \\ [(\hat{\mathbf{k}} \cdot \hat{\mathbf{k}}')\hat{\mathbf{k}}' \cdot \hat{\mathbf{z}}_n & (\hat{\mathbf{k}} \cdot \hat{\mathbf{k}}')[(\hat{\mathbf{k}} \cdot \hat{\mathbf{z}}_n)^2 + (\hat{\mathbf{k}}' \cdot \hat{\mathbf{z}}_n)^2] \\ -\hat{\mathbf{k}} \cdot \hat{\mathbf{z}}_n)(\hat{\mathbf{k}}' \times \hat{\mathbf{k}}) \cdot \hat{\mathbf{z}}_n & -[1 + (\hat{\mathbf{k}} \cdot \hat{\mathbf{k}}')^2][(\hat{\mathbf{k}} \cdot \hat{\mathbf{z}}_n)(\hat{\mathbf{k}}' \cdot \hat{\mathbf{z}}_n)] \end{pmatrix}, \end{aligned} \quad (17)$$

where the matrix elements of the first second-order term are

$$\begin{aligned} M_{11}^2 &= \{(\hat{\mathbf{k}}' \cdot \hat{\mathbf{k}})[(\hat{\mathbf{k}}' \times \hat{\mathbf{k}}) \cdot \hat{\mathbf{z}}_n]^2 \\ &\quad + [1 - (\hat{\mathbf{k}}' \cdot \hat{\mathbf{k}})^2](\hat{\mathbf{k}}' \cdot \hat{\mathbf{z}}_n)(\hat{\mathbf{k}} \cdot \hat{\mathbf{z}}_n)\}(\hat{\mathbf{k}}' \cdot \hat{\mathbf{k}})^{-1} \\ M_{12}^2 &= (\hat{\mathbf{k}}' \times \hat{\mathbf{k}}) \cdot \hat{\mathbf{z}}_n[(\hat{\mathbf{k}}' \cdot \hat{\mathbf{z}}_n) - (\hat{\mathbf{k}}' \cdot \hat{\mathbf{k}})(\hat{\mathbf{k}} \cdot \hat{\mathbf{z}}_n)] \\ M_{21}^2 &= (\hat{\mathbf{k}}' \times \hat{\mathbf{k}}) \cdot \hat{\mathbf{z}}_n[(\hat{\mathbf{k}} \cdot \hat{\mathbf{k}}')(\hat{\mathbf{k}}' \cdot \hat{\mathbf{z}}_n) - (\hat{\mathbf{k}} \cdot \hat{\mathbf{z}}_n)] \\ M_{22}^2 &= (\hat{\mathbf{k}}' \cdot \hat{\mathbf{k}})[(\hat{\mathbf{k}} \cdot \hat{\mathbf{z}}_n)^2 + (\hat{\mathbf{k}}' \cdot \hat{\mathbf{z}}_n)^2 \\ &\quad - 2(\hat{\mathbf{k}}' \cdot \hat{\mathbf{k}})(\hat{\mathbf{k}} \cdot \hat{\mathbf{z}}_n)(\hat{\mathbf{k}}' \cdot \hat{\mathbf{z}}_n)] \end{aligned} \quad (18)$$

and the matrix elements of the two third-order terms are

$$\begin{aligned} {}^1M_{11}^3 &= [(\hat{\mathbf{k}}' \times \hat{\mathbf{k}}) \cdot \hat{\mathbf{z}}_n]^3 \\ {}^1M_{12}^3 &= (\hat{\mathbf{k}}' \cdot \hat{\mathbf{z}}_n)(\hat{\mathbf{k}} \cdot \hat{\mathbf{z}}_n)^2[1 - (\hat{\mathbf{k}} \cdot \hat{\mathbf{k}}')^2] \\ &\quad + [(\hat{\mathbf{k}}' \times \hat{\mathbf{k}}) \cdot \hat{\mathbf{z}}_n]^2[\hat{\mathbf{k}}' \cdot \hat{\mathbf{z}}_n - (\hat{\mathbf{k}} \cdot \hat{\mathbf{z}}_n)(\hat{\mathbf{k}}' \cdot \hat{\mathbf{k}})] \\ {}^1M_{21}^3 &= -(\hat{\mathbf{k}}' \cdot \hat{\mathbf{z}}_n)^2(\hat{\mathbf{k}} \cdot \hat{\mathbf{z}}_n)[1 - (\hat{\mathbf{k}} \cdot \hat{\mathbf{k}}')^2] \\ &\quad + [(\hat{\mathbf{k}}' \times \hat{\mathbf{k}}) \cdot \hat{\mathbf{z}}_n]^2[-\hat{\mathbf{k}} \cdot \hat{\mathbf{z}}_n + (\hat{\mathbf{k}}' \cdot \hat{\mathbf{z}}_n)(\hat{\mathbf{k}}' \cdot \hat{\mathbf{k}})] \\ {}^1M_{22}^3 &= (\hat{\mathbf{k}}' \times \hat{\mathbf{k}}) \cdot \hat{\mathbf{z}}_n\{[(\hat{\mathbf{k}} \cdot \hat{\mathbf{z}}_n)^2 + (\hat{\mathbf{k}}' \cdot \hat{\mathbf{z}}_n)^2] \\ &\quad - 2(\hat{\mathbf{k}}' \cdot \hat{\mathbf{k}})(\hat{\mathbf{k}} \cdot \hat{\mathbf{z}}_n)(\hat{\mathbf{k}}' \cdot \hat{\mathbf{z}}_n)\}(\hat{\mathbf{k}}' \cdot \hat{\mathbf{k}}) \end{aligned} \quad (19)$$

and

$$\begin{aligned} {}^2M_{11}^3 &= (\hat{\mathbf{k}}' \times \hat{\mathbf{k}}) \cdot \hat{\mathbf{z}}_n[2(\hat{\mathbf{k}} \cdot \hat{\mathbf{k}}')(\hat{\mathbf{k}} \cdot \hat{\mathbf{z}}_n)(\hat{\mathbf{k}}' \cdot \hat{\mathbf{z}}_n) \\ &\quad - (\hat{\mathbf{k}} \cdot \hat{\mathbf{z}}_n)^2 - (\hat{\mathbf{k}}' \cdot \hat{\mathbf{z}}_n)^2] \\ {}^2M_{12}^3 &= -[(\hat{\mathbf{k}}' \times \hat{\mathbf{k}}) \cdot \hat{\mathbf{z}}_n]^2(\hat{\mathbf{k}} \cdot \hat{\mathbf{z}}_n)(\hat{\mathbf{k}}' \cdot \hat{\mathbf{k}}) \\ &\quad - (\hat{\mathbf{k}}' \cdot \hat{\mathbf{z}}_n)[(\hat{\mathbf{k}}' \cdot \hat{\mathbf{z}}_n) - (\hat{\mathbf{k}} \cdot \hat{\mathbf{z}}_n)(\hat{\mathbf{k}}' \cdot \hat{\mathbf{k}})]^2 \\ {}^2M_{21}^3 &= [(\hat{\mathbf{k}}' \times \hat{\mathbf{k}}) \cdot \hat{\mathbf{z}}_n]^2(\hat{\mathbf{k}}' \cdot \hat{\mathbf{z}}_n)(\hat{\mathbf{k}}' \cdot \hat{\mathbf{k}}) \\ &\quad + (\hat{\mathbf{k}} \cdot \hat{\mathbf{z}}_n)[(\hat{\mathbf{k}} \cdot \hat{\mathbf{z}}_n) - (\hat{\mathbf{k}}' \cdot \hat{\mathbf{z}}_n)(\hat{\mathbf{k}}' \cdot \hat{\mathbf{k}})]^2 \\ {}^2M_{22}^3 &= (\hat{\mathbf{k}}' \times \hat{\mathbf{k}}) \cdot \hat{\mathbf{z}}_n[(\hat{\mathbf{k}} \cdot \hat{\mathbf{z}}_n)^2 + (\hat{\mathbf{k}}' \cdot \hat{\mathbf{z}}_n)^2 \\ &\quad - 2(\hat{\mathbf{k}}' \cdot \hat{\mathbf{k}})(\hat{\mathbf{k}} \cdot \hat{\mathbf{z}}_n)(\hat{\mathbf{k}}' \cdot \hat{\mathbf{z}}_n)](\hat{\mathbf{k}}' \cdot \hat{\mathbf{k}}). \end{aligned} \quad (20)$$

We are now in a position to write an expression for the dependence of the quadrupole contribution on the individual components of the spin. In the same coordinate system as before, we obtain

$$\begin{aligned} f_{nE2}^{\text{XRES}} &= F_{E2}^{(0)} \begin{pmatrix} c_2 & 0 \\ 0 & c_2^2 \end{pmatrix} \\ &\quad + ic_2 F_{E2}^{(1)} \begin{pmatrix} z_2 t_2 & -z_1 c - z_3 s \\ -z_3 s + z_1 c & 2z_2 s_2 \end{pmatrix} \\ &\quad + (F_{E2}^{(2)} - F_{E2}^{(0)}) \begin{pmatrix} z_1^2 c^2 + z_2^2 c_2 - z_3^2 s^2 & -z_1 z_2 s c_2 + z_2 z_3 c c_2 \\ z_1 z_2 s c_2 + z_2 z_3 c c_2 & c_2^2(z_1^2 + z_3^2) \end{pmatrix} \\ &\quad + s_2 F_{E2}^{(2)} \begin{pmatrix} 0 & -z_1 z_2 c - z_2 z_3 s \\ z_1 z_2 c - z_2 z_3 s & -s_2(z_1^2 + z_3^2) \end{pmatrix} \\ &\quad + s_2 F_{E2}^{(0)} \begin{pmatrix} 0 & z_1 z_2 c + z_2 z_3 s \\ -z_1 z_2 c + z_2 z_3 s & -z_2^2 s_2 \end{pmatrix} \\ &\quad - i(F_{E2}^{(3)} - F_{E2}^{(1)}) \begin{pmatrix} -z_1^2 c^3 + z_1^2 z_3 s c^2 & z_1^3 c^3 + z_1^2 z_3 s c^2 \\ -z_1 z_3^2 s^2 c + z_1 z_2^2 s_2 s & -z_3 z_2^2 s_2 c - z_3^3 s^3 \\ -z_1^3 c^3 + z_1^2 z_3 s c^2 & -z_2 c_2 s_2(z_1^2 + z_3^2) \\ +z_1 z_3^2 s^2 c - z_1 z_2^2 s_2 s & \\ -z_3 z_2^2 s_2 c - z_3^3 s^3 & \end{pmatrix} \end{aligned}$$

$$\begin{aligned}
& -iF_{E2}^{(3)} \begin{pmatrix} z_2(z_1^2 + z_3^2)s_2 & -z_1z_2^2cc_2 \\ & +z_1^2z_3(s_2c + s^3) \\ & -z_2^2z_3c_2s \\ & -z_1z_3^2(c^3 + s_2s) \\ & -z_1^3cs^2 + z_3^3c^2s \end{pmatrix} \\
& +F_{E2}^{(4)} \begin{pmatrix} z_1z_2^2cc_2 & -z_2c_2s_2(z_1^2 + z_3^2) \\ & +z_1^2z_3(s_2c + s^3) \\ & -z_2^2z_3c_2s \\ & +z_1z_3^2(c^3 + s_2s) \\ & +z_1^3cs^2 + z_3^3c^2s \end{pmatrix}, \\
& \begin{pmatrix} z_1^2z_2^2c^2 - z_2^2z_3^2s^2 & z_1z_2z_3^2s^3 - z_1^3z_2sc^2 \\ & -z_2z_3^3cs^2 + z_1^2z_2z_3c^3 \\ -z_1z_2z_3^2s^3 + z_1^3z_2sc^2 & z_1^2z_3^2(c^4 + s^4) \\ -z_2z_3^3cs^2 + z_1^2z_2z_3c^3 & -(z_1^4 + z_3^4)s^2c^2 \end{pmatrix}, \quad (21)
\end{aligned}$$

where we have used the shorthand notation  $c = \cos \theta$ ,  $c_2 = \cos 2\theta$ ,  $c^2 = \cos^2 \theta$  etc. Despite the apparent complexity of (21), it can be of use in interpreting resonant scattering data. For example, in recent work on  $\text{Nd}_2\text{CuO}_4$ , a large resonant enhancement was observed at the  $\text{Nd } L_{\text{II}}$  edge (Hill, Vigliante, Gibbs, Peng & Greene, 1995). Polarization analysis of the scattering revealed it to be entirely  $\sigma \rightarrow \pi$  with little or no  $\sigma \rightarrow \sigma$  component. For the particular geometry of the experiment,  $z_1$ ,  $z_2$  and  $z_3 \neq 0$ . Inspection of (21) shows that in such a situation the observed scattering cannot be due to quadrupolar excitations, since  $\sigma \rightarrow \sigma$  is an allowed channel in the first-order terms. Therefore, the scattering is dipole and this in turn implies a polarization of the  $\text{Nd } 5d$  bands.

### 3. Examples

The expressions derived above are generally applicable. In order to illustrate their use, it is helpful to study some particular examples. We choose three magnetic structures common amongst the elemental rare earths.

#### 3.1. Basal-plane spiral antiferromagnet

We first take the case of a basal-plane spiral, such as occurs in  $\text{Ho}$ ,  $\text{Tb}$  and  $\text{Dy}$ . In this structure, the moments are confined to the  $ab$  plane in ferromagnetic sheets. The direction of the magnetization rotates from basal plane to basal plane, creating a spiral structure propagating along the  $c$  axis. The modulation vector then lies along  $(00L)$ . The magnetic moment takes the form

$$\hat{\mathbf{z}}_n = \cos(\boldsymbol{\tau} \cdot \mathbf{r}_n)\hat{\mathbf{U}}_1 + \sin(\boldsymbol{\tau} \cdot \mathbf{r}_n)\hat{\mathbf{U}}_2. \quad (22)$$

Now, the full X-ray scattering cross section may be written as

$$\begin{aligned}
d\sigma/d\Omega = \sum_{\lambda\lambda'} P_\lambda & \left| \langle \lambda' | \langle M_c \rangle | \lambda \rangle - i(\hbar\omega/mc^2) \langle \lambda' | \langle M_m \rangle | \lambda \rangle \right. \\
& \left. + \langle \lambda' | \langle M_{E1}^{\text{XRES}} \rangle | \lambda \rangle + \langle \lambda' | \langle M_{E2}^{\text{XRES}} \rangle | \lambda \rangle + \dots \right|^2, \quad (23)
\end{aligned}$$

where  $\lambda$ ,  $\lambda'$  are incident and scattered polarization states and  $P_\lambda$  is the probability for incident polarization  $\lambda$ .  $\langle M_c \rangle$  etc. are the expectation values of the respective operators in the initial and final state  $|a\rangle$  of the solid, i.e.  $\langle M_{E1}^{\text{XRES}} \rangle = \langle a | \sum_n \exp(i\mathbf{Q} \cdot \mathbf{r}_n) f_{nE1}^{\text{XRES}} | a \rangle$ . For the purposes of this example, we assume that the dipole contribution is dominant and ignore any interference effects. This will be valid at resonance and away from charge Bragg peaks, then

$$\begin{aligned}
M_{E1}^{\text{XRES}} = \sum_n \exp(i\mathbf{Q} \cdot \mathbf{r}_n) \\
\times \begin{pmatrix} z_2^2 F^{(2)} & -iz_1 \cos \theta F^{(1)} - z_2 z_1 \sin \theta F^{(2)} \\ iz_1 \cos \theta F^{(1)} + z_2 z_1 \sin \theta F^{(2)} & iz_2 \sin 2\theta F^{(1)} - z_1^2 \sin^2 \theta F^{(2)} \end{pmatrix}. \quad (24)
\end{aligned}$$

For simplicity, we take  $P_\lambda = \delta_{\lambda\sigma}$ , which is a reasonable approximation for a bending magnet source at a synchrotron, then only  $\sigma \rightarrow \sigma$  and  $\sigma \rightarrow \pi$  terms contribute and

$$\begin{aligned}
d\sigma/d\Omega = & \left| \langle a | \sum_n \exp(i\mathbf{Q} \cdot \mathbf{r}_n) z_2^2 F^{(2)} | a \rangle \right|^2 \\
& + \left| \langle a | \sum_n \exp(i\mathbf{Q} \cdot \mathbf{r}_n) (iz_1 \cos \theta F^{(1)} \right. \\
& \left. + z_2 z_1 \sin \theta F^{(2)}) | a \rangle \right|^2. \quad (25)
\end{aligned}$$

Substituting  $z_1 = \cos(\boldsymbol{\tau} \cdot \mathbf{r}_n)$ ,  $z_2 = \sin(\boldsymbol{\tau} \cdot \mathbf{r}_n)$  and writing the sine and cosine terms as the sums of complex exponentials, we obtain the cross section for a flat spiral with incident radiation perfectly polarized perpendicular to the scattering plane:

$$\begin{aligned}
d\sigma/d\Omega|_{E1}^{\text{XRES}} = & \frac{1}{4} F^{2(2)} \delta(\mathbf{Q} - \mathbf{G}) \\
& + \frac{1}{4} \cos^2 \theta F^{2(1)} (\mathbf{Q} - \mathbf{G} \pm \boldsymbol{\tau}) \\
& + \frac{1}{16} (1 + \sin^2 \theta) F^{2(2)} \delta(\mathbf{Q} - \mathbf{G} \pm 2\boldsymbol{\tau}). \quad (26)
\end{aligned}$$

The intensity of the observed scattering will only be proportional to the expression above if both polarization components of the scattered beam are collected with equal weight. This is the case if no analyzer crystal is employed. If one is used, then the polarization component that is in the scattering plane of the analyzer must be weighted by a factor  $\cos^2 2\theta_A$ , where  $\theta_A$  is the Bragg angle of the analyzer crystal. From (26), we see that, in addition to producing scattering at the Bragg peak, the resonant dipole contribution produces two magnetic satellites at  $\pm\boldsymbol{\tau}$  and  $\pm 2\boldsymbol{\tau}$  on either side of the Bragg peak. We may calculate (Pengra *et al.*, 1994) the ratio of the factors  $F^{(1)}/F^{(2)}$  in  $\text{Ho}$  using the published value for the ratio of the first two resonant harmonics (Gibbs *et al.*, 1991) and (26),

$$\frac{I(0, 0, 2 + \boldsymbol{\tau})}{I(0, 0, 2 + 2\boldsymbol{\tau})} = \left( \frac{2F^{(1)}}{F^{(2)}} \right)^2 \frac{\cos^2 \theta}{(1 + \sin^2 \theta)} \simeq 30 \quad (27)$$

$$\Rightarrow F^{(1)}/F^{(2)} \simeq 2.7. \quad (28)$$

As we shall see in the next example, knowledge of this ratio allows one to calculate relative intensities of resonant peaks in Ho for structures other than a basal-plane spiral.

We shall now briefly consider the contribution to the scattering from the  $E2$  resonant process. From inspection of (21), it can be seen that, in the  $\sigma$ -to- $\pi$  channel, the  $E2$  resonance produces satellites not only at the first harmonic [second term of (21)] and second-harmonic satellites (third, fourth and fifth terms) as was shown to be the case for the  $E1$  resonance, but also at the third (sixth and seventh terms) and fourth (eighth term) harmonics. These additional peaks have been observed in Ho (Gibbs *et al.*, 1988, 1991) and already discussed in terms of electric multipole transitions (Hannon *et al.*, 1988). It is interesting to note that no report has yet been made of higher harmonics in the magnetic scattering from Ho not arising from the cross section. At low temperatures, the moments in Ho bunch around the nearest easy axis in the hexagonal basal planes, which gives rise to intense fifth and seventh harmonics in neutron scattering experiments. Given the signal-to-noise ratio routinely achievable at a synchrotron, we suggest that these harmonics should be observable with X-rays.

### 3.2. $c$ -axis conical spiral

In this example, we treat the case in which moments are tilted at an angle  $\alpha$  to the  $c$  axis, in addition to spiraling around the  $c$  axis. Such a conical phase occurs in Ho and Er at low temperatures. In this case,

$$\hat{\mathbf{z}}_n = \sin \alpha \cos(\boldsymbol{\tau} \cdot \mathbf{r}_n) \hat{\mathbf{U}}_1 + \sin \alpha \sin(\boldsymbol{\tau} \cdot \mathbf{r}_n) \hat{\mathbf{U}}_2 + \cos \alpha \hat{\mathbf{U}}_3. \quad (29)$$

For simplicity, we consider only the  $\sigma \rightarrow \pi$  dipole scattering. This would be measured in an experiment in which a polarization analyzer was employed to select only such rotated components of the scattering beam. In this case,

$$f_{nE1}^{\sigma \rightarrow \pi} = -i \cos \alpha \sin \theta F^{(1)} + [(i \cos \theta \sin \alpha)/2](F^{(1)} \mp \cos \alpha F^{(2)}) \exp(\pm i \boldsymbol{\tau} \cdot \mathbf{r}_n) \mp [(i \sin \theta \sin^2 \alpha)/4] F^{(2)} \exp(\pm i 2 \boldsymbol{\tau} \cdot \mathbf{r}_n). \quad (30)$$

Note that here the presence of a  $c$ -axis component to the magnetic moment that is not modulated produces a 'mixing' of the terms, that is some 'second-order' terms,  $F^{(2)}$ , contribute to the first-harmonic satellite.

Further, as noted by Pengra *et al.* (1994), the intensity of the first harmonic has a maximum as a function of the tilt angle  $\alpha$ . The amplitude of the scattering at  $\boldsymbol{\tau}$ ,  $A_\tau$ , is

$$A_\tau = A' \sin \alpha (F^{(1)} \mp \cos \alpha F^{(2)}), \quad (31)$$

$$\partial A_\tau / \partial \alpha = 0 \Rightarrow \cos \alpha / \cos 2\alpha = \mp F^{(2)} / F^{(1)}. \quad (32)$$

Substituting  $F^{(2)}/F^{(1)} = 2.7$  for Ho, we obtain  $\alpha_{\max} =$

72.5°, the tilt angle for which the maximum diffracted intensity at the  $\boldsymbol{\tau}$  satellite would be observed. Hence, one can, in principle, obtain information regarding spin reorientation transitions from resonant intensity data.

### 3.3. $c$ -axis modulated structures

The rare earths Er and Tm form  $c$ -axis modulated (CAM) structures. In these phases, the direction of the moment is aligned along the  $c$  axis of the h.c.p. structure and the magnetic moment is sinusoidally modulated, with wave vector  $\boldsymbol{\tau}$ . The resonant scattering from such phases was first discussed by Bohr, Gibbs & Huang (1990). For the CAM structure,

$$\hat{\mathbf{z}}_n = \sin(\boldsymbol{\tau} \cdot \mathbf{r}_n) \hat{\mathbf{U}}_3 \quad (33)$$

and the cross section greatly simplifies. For a  $\sigma$ -polarized incident beam at a dipole resonance, then only the first resonant harmonic is seen along the (00L) direction. The scattering amplitude is

$$A = \sum_n \exp(i \mathbf{Q} \cdot \mathbf{r}_n) [-i F^{(1)} \sin \theta \sin(\boldsymbol{\tau} \cdot \mathbf{r}_n)] \quad (34)$$

and the observed intensity is therefore

$$I = F^{2(1)} [(\sin^2 \theta)/4] \delta(\mathbf{Q} - \mathbf{G} \pm \boldsymbol{\tau}). \quad (35)$$

All of the scattering is of the type  $\sigma \rightarrow \pi$ . The presence of quadrupole contributions will give rise to additional harmonics at  $\pm 2\boldsymbol{\tau}(\sigma \rightarrow \sigma)$  and  $\pm 3\boldsymbol{\tau}(\sigma \rightarrow \pi)$ . However, there are no  $E1$  or  $E2$  fourth-harmonic satellites for the CAM structure along (00L) for purely  $\sigma$ -polarized incident light.

Both Er (Sanyal, Gibbs, Bohr & Wulff, 1994; Helgesen, Hill, Thurston & Gibbs, 1995) and Tm (Bohr, Gibbs & Huang, 1990; Helgesen, Hill, Thurston & Gibbs, 1995) have been investigated using resonant X-ray magnetic scattering. Bohr *et al.* (1990) found that the first harmonic of Tm exhibited only  $\sigma \rightarrow \pi$  scattering at the  $L_{\text{III}}$ -absorption edge, consistent with the above analysis. Further, no third harmonic was seen. However, second and fourth charge harmonics were observed, arising from lattice modulations. These obscured the investigation of any resonant harmonics at these positions. Similar results were obtained for Er (Sanyal *et al.*, 1994; Helgesen, Hill, Thurston & Gibbs, 1995). However, in this case a third harmonic was observed (Helgesen, Hill, Thurston & Gibbs, 1995). Based on relative intensities, the authors attributed this harmonic to a magnetic structural peak arising from a non-sinusoidal modulation and not a quadrupolar contribution. We conclude that the scattering observed from CAMs is consistent with that expected from the single-electron approximation of Hannon *et al.* (1988).

#### 4. Correlation functions

The importance of X-ray scattering as a probe of condensed-matter systems arises from the connection between the scattering cross section and calculable correlation functions. For charge scattering from atomic electrons, the cross section is proportional to the Fourier transform of the equal-time electron-density–electron-density correlation function  $\langle \rho(\mathbf{r})\rho(\mathbf{0}) \rangle$ . The goal of this section is to calculate similar relations for resonant scattering. In order to do so, we will use a restricted set of the generalized functions of Luo, Trammel & Hannon (1993), following an approach of Hamrick (1994). This has the advantage of deriving correlation functions in terms of intuitive quantities. However, as a result of the approximations used, the analysis is restricted to elastic scattering. Therefore, the correlation functions derived are static ones and not the usual instantaneous correlation functions of quasi-elastic X-ray scattering. Nevertheless, this approach is useful since the difference between elastic scattering and quasi-elastic scattering is typically only of importance in the vicinity of a second-order phase transition, where the dynamic fluctuations become important. Further, static disorder is often of great interest and thus a mathematical basis for analysis of peak line shapes is of some utility. Finally, differences in the temperature dependence of Bragg elastic scattering at the different harmonics in the elemental rare earths (Helgesen *et al.*, 1994, 1995) may be explained by such an approach.

The initial part of the derivation follows the work of Luo *et al.* (Luo, Trammel & Hannon, 1993; Luo, 1994) and Hamrick (1994), which we then extend to obtain the correlation functions. Although none of the mathematics of this section are new, the final relationships are sufficiently useful to warrant inclusion in this paper. In order to obtain such expressions, one is required to make some approximations and generality is necessarily lost. The assumptions chosen are reasonable for the particular case of the rare earths. Care must be taken in using the derived expressions outside their range of validity.

In this section of the paper, we are no longer concerned with the polarization dependences and it is convenient to collect them into a single term,  $P^*$ . The cross section, for pure electric multipole transitions (*i.e.*  $L' = L$ ) may be written

$$f_{\text{EL}}^e(\omega) = (4\pi/|k|)f_D \sum_{MM'} F_{LM';LM}(\omega) P_{LM';LM}^*(\hat{\epsilon}^*, \hat{\mathbf{k}}'; \hat{\epsilon}, \hat{\mathbf{k}}), \quad (36)$$

where

$$P_{LM';LM}^*(\hat{\epsilon}^*, \hat{\mathbf{k}}'; \hat{\epsilon}, \hat{\mathbf{k}}) = \hat{\epsilon}^* \cdot \mathbf{Y}_{LM'}^{(e)}(\hat{\mathbf{k}}') \mathbf{Y}_{LM}^{(e)*}(\hat{\mathbf{k}}) \cdot \hat{\epsilon}. \quad (37)$$

Here,  $L = 1$  and  $2$  for electric dipole and quadrupole transitions, respectively, and  $\mathbf{k} = |\mathbf{k}_i| = |\mathbf{k}_f|$  is the momentum of the photon. As before [(3)], it simplifies matters to restrict ourselves to transitions for which

$M' = M$ . If the system is invariant to rotations about an axis parallel to the local field direction, then such transitions are the only ones allowed by azimuthal symmetry. In fact, even if azimuthal symmetry is broken, one may still expect  $M' = M$  to hold, at least approximately, if the exchange interaction dominates crystal-field effects. Also, for dipole transitions, the same restriction holds even for strong crystal fields if the point group is  $C_3$ ,  $C_4$  or  $C_6$  (Hamrick, 1994). Note that, in this formalism, scattering events in which the value of  $J_z$  is altered are not permitted and therefore only a limited set of inelastic fluctuations (for example those in  $J_x$  and  $J_y$ ) will be contained in any correlation function derived from these operators. Rather than derive a dynamic structure factor that does not include all possible fluctuations, we have chosen to restrict the analysis to the purely elastic case, as mentioned in the beginning of this section. Following Hamrick (1994), we decompose the coefficients  $F_{LM}$  into a resonant piece and an amplitude coefficient,  $A_{q0}$ . For clarity, the sum  $\sum_{M=-L}^L$  is written  $\sum_{q=0}^{2L}$  so that  $q = 1$  corresponds to scattering at the first harmonic of an incommensurate structure,  $q = 2$  at the second harmonic and so on. Then,

$$f_{\text{EL}}^{(e)}(\omega) = \sum_{q=0}^{2L} \left( \sum_{\text{resonances}} (\lambda/\lambda_{\text{res}}) \{r_0/[x_{\text{res}}(\omega) - i]\} A_{q0}^{(\text{EL})} \right) \times P^*(\hat{\epsilon}^*, \hat{\mathbf{k}}'; \hat{\epsilon}, \hat{\mathbf{k}}) \quad (38)$$

with

$$A_{q0}^{(\text{EL})} = [mc^2/(\Gamma_{\text{res}}/2)] 4\pi[(L+1)(2L+1)/L] \times \{1/[(2L+1)!!]^2\} [(2l+1)/(2l'+1)] \times (ka_0)^{2L} |R_h|(r/a_0)^L |R_v|^2 \times C^2(l, L, l'; 0, 0, 0) C_{q0}^{(\text{EL})}(l'; lj), \quad (39)$$

where  $x_{\text{res}} = (E_c - E_i - \hbar\omega)/\Gamma_c/2$  is the deviation from resonance in units of the half-width of the excited state and  $|R_h\rangle$  and  $|R_v\rangle$  are single-electron hole and valence wave functions.  $C(j_1, j_2, j_3; m_1, m_2, m_3)$  is a Clebsch–Gordon coefficient and  $C_{q0}$  the amplitude. The great contribution of Luo, Trammel & Hannon (1993) and independently Carra and co-workers (Carra, Thole, Altarelli & Wang, 1993; Carra, König, Thole & Altarelli, 1993; Carra & Thole, 1994) was to express the amplitude coefficients  $C_{q0}$  in terms of experimentally significant quantities, the electron spin and orbital moments. This procedure is valid within the fast-collision approximation. That is, when either the deviation from resonance,  $\Delta\omega = E_c - E_a - \hbar\omega$ , or the width,  $\Gamma_c$ , is large compared to the splitting of the excited-state configuration. This approximation is expected to hold for the  $L_{\text{II}}$  and  $L_{\text{III}}$  edges of the rare earths and actinides and for the  $M_{\text{IV}}$  and  $M_{\text{V}}$  edges of the actinides. In this regime, the resonant factors can be summed independently leaving amplitude coefficients that may be written in terms of multipole

moment operators, which are themselves single-particle operators summed over the valence electrons in the initial state. These effective scattering operators,  $M_{q_0}^{(\text{EL})}$ , are related to the amplitude coefficients by (Hamrick, 1994)

$$C_{q_0}^{(\text{EL})} = (-1)^{L-q} [(2L+1)/(2q+1)]^{1/2} \langle \psi | M_{q_0}^{(\text{EL})} | \psi \rangle, \quad (40)$$

where  $|\psi\rangle$  is the many-electron wave function of the ion. For electric dipole transitions (Luo, Trammel & Hannon, 1993),

$$M_0^{(E1)} = [(j \pm 1/2)/(2l+1)] \alpha_0 N_h \mp \gamma_0 \sum_i \mathbf{s}_i \cdot \mathbf{l}_i \quad (41)$$

$$M_1^{(E1)} = [(j \pm 1/2)/(2l+1)] \alpha_1 \mathbf{L} \pm \beta_1 \mathbf{S} \\ \pm \gamma_1 \sum_i [\mathbf{s}_i - 3\{\mathbf{s}_i \cdot \mathbf{l}_i, \mathbf{l}_i\}/2l'(l'+1)] \quad (42)$$

$$M_2^{(E1)} = -[(j \pm 1/2)/(2l+1)] \alpha_2 \sum_i V^{(2)}(\mathbf{l}_i \otimes \mathbf{l}_i) \\ \pm \beta_2 \sum_i V^{(2)}(\mathbf{s}_i \otimes \mathbf{l}_i) \\ \pm \gamma_2 \sum_i V^{(2)}[\mathbf{s}_i \otimes V^{(3)}(\mathbf{l}_i \otimes \mathbf{l}_i \otimes \mathbf{l}_i)], \quad (43)$$

where the coefficients  $\alpha_q$ ,  $\beta_q$  and  $\gamma_q$  depend only on  $L$ ,  $l$  and  $l'$ .  $N_h$  is the number of holes per ion. The expression  $V^{(R)}(X \otimes Y)$  refers to a tensor of rank  $R$  constructed from tensors  $X$  and  $Y$  and the sum over  $i$  runs over the valence electrons. For quadrupole transitions, the first three operators have a similar form, differing only in the coefficients  $\alpha_q$ ,  $\beta_q$  and  $\gamma_q$ . Luo (1994) derives complete expressions for  $M_{q=0 \rightarrow 4}^{(E2)}$ . Hamrick (1994) then uses the Wigner-Eckart theorem to re-express the effective scattering operators in terms of a new operator,  $\mathcal{J}_{q_0}$ , derived from  $J$ , the total-angular-momentum quantum number. This is permissible if  $J$  is a good quantum number and again this is generally true for the rare earths. Then (Hamrick, 1994),

$$C_{q_0}^{(\text{EL})}(l'; lj) = [\xi_{q_0}^{(\text{EL})}(l'; l) \pm \eta_{q_0}^{(\text{EL})}(l'; l)] \langle \mathcal{J}_{q_0} \rangle, \quad (44)$$

where  $\xi$  and  $\eta$  are temperature-independent constants and the  $\pm$  corresponds to  $j = l \pm 1/2$ . The new operators  $\mathcal{J}_{q_0}$  are given by

$$\begin{aligned} \mathcal{J}_{00} &= 1 \\ \mathcal{J}_{10} &= J_z \\ \mathcal{J}_{20} &= 3J_z^2 - J(J+1) \\ \mathcal{J}_{30} &= 5J_z^3 - 3J_z J(J+1) + J_z \\ \mathcal{J}_{40} &= 35J_z^4 - 30J_z^2 J(J+1) + 3J^2(J+1)^2 \\ &\quad + 25J_z^2 - 6J(J+1). \end{aligned} \quad (45)$$

In order to calculate the measured correlation function for scattering from a solid, we make the assumptions that the only difference from site to site is the effective scattering operator,  $\mathcal{J}_{q_0}$ , and that all other terms in (38) are constant across the solid. In this case, we may subsume all the resonance and polarization factors, and

other constants, into an overall amplitude factor  $\mathcal{A}$  such that the scattering operator for a given site,  $n$ , is

$$f_n^{(\text{EL})} = \mathcal{A} \sum_{q=0}^{2L} \mathcal{J}_{q_0}. \quad (46)$$

One may now follow the usual route to obtain the measured correlation function from a given scattering operator. For completeness, we reproduce it below. The double differential scattering cross section is, in general,

$$d^2\sigma/d\Omega dE_f = \sum_{i,f} P_i |\langle f | \sum_n f_n \exp(i\mathbf{Q} \cdot \mathbf{r}_n) | i \rangle|^2 \\ \times \delta(\hbar\omega + E_i - E_f), \quad (47)$$

where the  $\sum_f$  arises because X-ray scattering is not sensitive to the final state of the solid and  $P_i$  is the probability that the system is in the initial state  $|i\rangle$ . Using the completeness of the final states,  $\sum_f |f\rangle \langle f| = 1$  and the constraint that  $E_i = E_f$ , we obtain

$$d^2\sigma/d\Omega dE = \sum_i P_i \langle i | f(\mathbf{Q}) f(-\mathbf{Q}) | i \rangle \delta(\hbar\omega). \quad (48)$$

With the definition  $\langle O \rangle = \sum_i P_i \langle i | O | i \rangle$ , for any operator  $O$ , then, integrating over energy, we get

$$(d\sigma/d\Omega)_{\text{elastic}} \propto \langle f(\mathbf{Q}) f(-\mathbf{Q}) \rangle. \quad (49)$$

Elastic scattering is sensitive to the static correlations, that is the correlation function may be more properly written

$$(d\sigma/d\Omega)_{\text{elastic}} \propto \langle f(\mathbf{Q}) f(-\mathbf{Q}, t = \infty) \rangle. \quad (50)$$

For the case of an incommensurate magnetic structure, the dipole scattering from each term in the series,  $q = 0, 1, 2$ , appears at a different point in reciprocal space and there is no interference. In this case, the cross section further simplifies to

$$(d\sigma/d\Omega)^{(E1)} \propto \langle \mathcal{J}_{00}(\mathbf{Q}) \mathcal{J}_{00}(-\mathbf{Q}, \infty) \rangle \\ + \langle \mathcal{J}_{10}(\mathbf{Q}) \mathcal{J}_{10}(-\mathbf{Q}, \infty) \rangle \\ + \langle \mathcal{J}_{20}(\mathbf{Q}) \mathcal{J}_{20}(-\mathbf{Q}, \infty) \rangle. \quad (51)$$

Substituting (45) produces the important result that, at the first dipole resonant harmonic of an incommensurate magnet, the scattering is proportional to the correlation function  $\langle J_z(\mathbf{Q}) J_z(-\mathbf{Q}, \infty) \rangle$ . The  $q = 1$  quadrupole term has a similar form and so will measure the same correlation function. Higher-order harmonics will measure slightly more complex correlation functions, as given by (45) and (51).

## 5. Summary

We have reformulated the X-ray resonant exchange scattering cross section in terms of linear polarization states. This allows for the presentation of the cross section in a simple matrix form such that the polarization dependences and the dependence of the scattering on the

individual components of the magnetic moment becomes explicit. This process was carried out for the experimentally important cases of electric dipole and quadrupole transitions. This formulation provides for the straightforward interpretation of magnetic diffraction patterns in terms of the components of the magnetic moment. Examples are given of the calculated diffraction patterns from some simple magnetic structures.

The appearance of higher-order moments in the cross section generates resonant harmonics, distinct from any structural harmonics that may or may not be present. It is an interesting question as to what magnetic properties are being measured at such resonant harmonics. In the second half of this paper, the measured correlation functions are derived under certain assumptions. We find that the scattering at the position of the first harmonic in an incommensurate system is proportional to the spin-spin correlation function  $\langle J_z(\mathbf{Q})J_z(-\mathbf{Q}, \infty) \rangle$  while, at the position of higher harmonics, the scattering probes higher-order correlation functions.

It is a pleasure to acknowledge stimulating and useful discussions with N. Bernhoeft, M. Blume and D. Gibbs. The work at Brookhaven National Laboratory was carried out under contract no. DE-AC02-76CH00016, Division of Materials Science, US Department of Energy.

#### References

- Berestetskii, V. B., Lifshitz, E. M. & Pitaevskii, L. P. (1971). *Relativistic Quantum Theory*. New York: Pergamon Press.
- Bergevin, F. de & Brunel, M. (1981). *Acta Cryst.* **A37**, 314–324.
- Bergevin, F. de, Brunel, M., Galera, R. M., Vettier, C., Elkaim, E., Bessiere, M. & Lefebvre, S. (1992). *Phys. Rev. Lett.* **46**, 10772–10776.
- Blume, M. (1985). *J. Appl. Phys.* **57**, 3615–3618.
- Blume, M. (1994). Proceedings of the 2nd International Conference on Anomalous Scattering.
- Blume, M. & Gibbs, D. (1988). *Phys. Rev. B*, **37**, 1779–1789.
- Bohr, J., Gibbs, D. & Huang, K. (1990). *Phys. Rev. B*, **42**, 4322–4328.
- Carra, P., König, H., Thole, B. T. & Altarelli, M. (1993). *Physica (Utrecht)*, **B192**, 182–190.
- Carra, P. & Thole, B. T. (1994). *Rev. Mod. Phys.* **66**, 1509–1515.
- Carra, P., Thole, B. T., Altarelli, M. & Wang, X. (1993). *Phys. Rev. Lett.* **70**, 694–697.
- Finkelstein, K. D., Hamrick, M. & Shen, Q. (1993). Proceedings of the ICAS Conference.
- Finkelstein, K. D., Shen, Q. & Shastri, S. (1992). *Phys. Rev. Lett.* **69**, 1612–1615.
- Gibbs, D., Grübel, G., Harshmann, D. R., Isaacs, E. D., McWhan, D. B., Mills, D. & Vettier, C. (1991). *Phys. Rev. B*, **43**, 5663–5681.
- Gibbs, D., Harshmann, D. R., Isaacs, E. D., McWhan, D. B., Mills, D. & Vettier, C. (1988). *Phys. Rev. Lett.* **61**, 1241–1244.
- Hamrick, M. (1990). Master's thesis, Rice University, USA.
- Hamrick, M. (1994). PhD thesis, Rice University, USA.
- Hannon, J. P., Trammel, G. T., Blume, M. & Gibbs, D. (1988). *Phys. Rev. Lett.* **61**, 1245.
- Helgeson, G., Hill, J. P., Thurston, T. R. & Gibbs, D. (1995). *Phys. Rev. B*, **52**, 9446–9454.
- Helgeson, G., Hill, J. P., Thurston, T. R., Gibbs, D., Kwo, J. & Hong, M. (1994). *Phys. Rev. B*, **50**, 2990–3004.
- Hill, J. P., Vigliante, A., Gibbs, D., Peng, J. L. & Greene, R. L. (1995). *Phys. Rev. B*, **52**, 6575–6580.
- Isaacs, E. D., McWhan, D. B., Kleinman, R. N., Bishop, D. J., Ice, G. E., Zschack, P., Gaulin, B. D., Mason, T. E., Garrett, J. D. & Buyers, W. J. L. (1990). *Phys. Rev. Lett.* **65**, 3185–3188.
- Isaacs, E. D., McWhan, D. B., Peters, C., Ice, G. E., Siddons, D. P., Hastings, J. B., Vettier, C. & Vogt, O. (1989). *Phys. Rev. Lett.* **62**, 1671–1674.
- Luo, J. (1994). PhD thesis, Rice University, USA.
- Luo, J., Trammel, G. T. & Hannon, J. P. (1993). *Phys. Rev. Lett.* **71**, 287–290.
- Pengra, D. B., Thoft, N. B., Wulff, M., Feidenhans'l, R. & Bohr, J. (1994). *J. Phys. Condens. Matter*, **6**, 2409–2422.
- Rennert, P. (1993). *Phys. Rev. B*, **48**, 13559–13568.
- Sanyal, M. K., Gibbs, D., Bohr, J. & Wulff, M. (1994). *Phys. Rev. B*, **49**, 1079–1085.
- Tang, C. C., Stirling, W. G., Lander, G. H., Gibbs, D., Herzog, W., Carra, P., Thole, B. T., Mattenberger, K. & Vogt, O. (1992). *Phys. Rev. B*, **46**, 5287–5297.
- Thurston, T. R., Helgeson, G., Gibbs, D., Hill, J. P., Gaulin, B. D. & Shirane, G. (1993). *Phys. Rev. Lett.* **70**, 3151–3154.
- Trammel, G. T. (1962). *Phys. Rev.* **126**, 1045–1054.
- Trammel, G. T. & Hannon, J. P. (1969). *Phys. Rev.* **186**, 306–325.